

Diagnostic nomogram for gallbladder wall thickening mimicking malignancy: using contrast-enhanced ultrasonography or multi-detector computed tomography?

Li-Da Chen,¹ Yang Huang,¹ Xiao-Hua Xie,¹ Wei Chen,² Quan-Yuan Shan,¹ Ming Xu,¹ Jin-Ya Liu,¹ Zhi-Qiang Nie,³ Xiao-Yan Xie,¹ Ming-De Lu,^{1,2} Shun-Li Shen,² Wei Wang¹

¹Department of Medical Ultrasonics, Institute of Diagnostic and Interventional Ultrasound, The First Affiliated Hospital of Sun Yat-Sen University, 58 Zhongshan Road 2, Guangzhou 510080, China

²Department of Hepatobiliary Surgery, The First Affiliated Hospital of Sun Yat-Sen University, Guangzhou, China

³Department of Epidemiology, Guangdong Cardiovascular Institute, Guangdong General Hospital, Guangdong Academic of Medical Science, Guangzhou, China

Abstract

Objectives: To establish a diagnostic nomogram using contrast-enhanced ultrasonography (CEUS) in gallbladder wall thickening mimicking malignancy and compare with multi-detector computed tomography (MDCT).

Methods: Seventy-two patients with gallbladder wall thickening on B-mode ultrasonography (BUS) were examined by CEUS to develop independent predictors for diagnosing gallbladder carcinoma. Among the 72 cases, 48 patients underwent both CEUS and MDCT. The diagnostic performances of different sets of CEUS criteria and MDCT were compared. A prediction model of malignancy using CEUS was developed. The performance of the nomogram was assessed with respect to its calibration, discrimination, and clinical usefulness.

Results: Multivariate logistic regression indicated that inhomogeneous enhancement in the arterial phase was the strongest independent predictor of malignancy (odds ratio, OR 51.162), followed by interrupted inner layer (OR 19.788), washout time ≤ 40 s (OR 16.686), and wall thickness > 1.6 cm (OR 3.019), which were all selected into the nomogram. Combined with the above significant features, the diagnostic performance of CEUS (AUC = 0.917) was higher than that of MDCT

(AUC = 0.788, $P = 0.070$). The predictive model using CEUS showed good discrimination, with a concordance index of 0.974 (0.950 through internal validation), and good calibration. Decision curve analysis demonstrated that the nomogram was clinically useful.

Conclusions: CEUS could accurately differentiate between malignant and benign gallbladder wall thickening with equivalent efficacy compared to MDCT. The proposed nomogram could be conveniently used to facilitate the preoperative individualized prediction of malignancy in patients with gallbladder wall thickening.

Key words: Gallbladder—Neoplasm—Contrast-enhanced ultrasonography—Multi-detector computed tomography—Nomogram

Gallbladder carcinoma, the most common biliary tract cancer, is traditionally regarded as a highly lethal disease with an overall 5-year survival of less than 5% [1]. The prognosis of gallbladder carcinoma remains poor because of nonspecific symptoms or asymptomatic presentation unless the cancer invades adjacent organs [2, 3]. At this stage, surgical intervention is no longer effective and a mass-like lesion may be formed to replace the gallbladder and extends into the liver [4].

At the early stage of gallbladder carcinoma, thickening of the wall may be the only detectable imaging sign [3]. B-mode ultrasonography (BUS) has been applied as the screening method for patients with upper abdominal

Electronic supplementary material The online version of this article (doi:10.1007/s00261-017-1162-z) contains supplementary material, which is available to authorized users.

Correspondence to: Shun-Li Shen; email: beyondjulian@163.com; Wei Wang; email: wangw73@mail.sysu.edu.cn

pain and jaundice [5]. In clinical settings, however, gallbladder wall thickening can also occur in a wide range of benign diseases, such as cholecystitis, adenomyomatosis, and hypoalbuminemia [6]. Most benign wall thickening can be confirmed if the gallbladder wall is regularly thickened with clear layering. However, making a precise preoperative diagnosis may be difficult when the images mimic malignancy, such as in focal, asymmetrical or irregular thickening of the wall visualized by BUS. Because there is no specific tumor marker on serological examination [6], an additional technology such as computed tomography (CT) and endoscopic US would be helpful for differentiation [7, 8]. Although superior to trans-abdominal US and CT, endoscopic US is more invasive than transcutaneous ultrasound, and takes longer time with sedation [9–11]. Final diagnosis was most frequently dependent on CT because it allows enhanced visualization of the gallbladder lesions [3, 12, 13].

The use of contrast-enhanced ultrasonography (CEUS) in gallbladder diseases, a modality that can reveal the macro- and microcirculation of gallbladder lesions, is at early stage with limited experience [14]. The role of CEUS in gallbladder diseases still remains unclear [15–18]. Because the blood supply of gallbladder is provided entirely by the cystic artery without portal vein branches, the vascular phases of the gallbladder are different from those of the liver. [19]. In other words, hyper-enhancement in the arterial phase with washout cannot provide sufficient information to distinguish between malignant and benign gallbladder diseases [20]. However, other characteristics such as vascularity, enhancement time, and washout time may be helpful for differentiation due to real-time scanning in CEUS.

To our knowledge, no study has assessed the value of CEUS in the diagnosis of gallbladder wall thickening compared with CT. In this study, we proposed a CEUS diagnostic nomogram for irregular gallbladder wall thickening diseases suspected to be malignancies by BUS, aiming to retrospectively compare the diagnostic tests of CEUS and CT.

Methods

Study populations

This retrospective study was approved by the Institutional Review Board of the First Affiliated Hospital of Sun Yat-Sen University, and informed consent was obtained from all of the patients. From July 2005 to Aug 2015, we enrolled 82 patients who had focal or irregular thickening of gallbladder wall and underwent both BUS and CEUS. The inclusion criteria were as follows: (1) imaging on BUS showed focal ($n = 5$) or irregular ($n = 77$) gallbladder wall thickening (≥ 0.4 cm); (2) cases who received both BUS and CEUS examinations; and (3) all cases were confirmed by pathologic examination after surgery. Exclusion criteria included (1) an intraluminal polypoid nodula without wall thickening on BUS; (2) a mass formation replacing the gallbladder with disappearance of the lumen and the wall of gallbladder; (3) metastases in liver or lymph node were visible on the CT or US ($n = 2$); (4) recent coronary syndrome, pregnancy or lactation, age < 18 years or > 80 years. A total of 72 patients were finally included (Table 1) in the CEUS imaging analysis. Among the 72 cases, there were 48 patients also underwent multi-detector CT (MDCT) in our institution within 2 weeks before or after CEUS

Table 1. Ultrasound features of gallbladder wall-thickening

	Benign ($n = 39$)	Malignant ($n = 33$)	<i>P</i>
Basic characteristics			
Gender (female/male)	15/24	11/22	0.652
Age (years)†	54 ± 12 (32–80)	64 ± 11 (28–80)	0.001*
CA 19-9 > 35 (U/mL)	12.0 (30.8)	17.0 (51.5)	0.074
Wall thickness (cm)†	1.2 ± 0.4 (0.7–2.5)	1.9 ± 0.7 (0.8–4.0)	<.001*
BUS			
Cholelithiasis	19 (48.7)	12 (36.4)	0.291
Interruption of the inner layer	20 (51.3)	30 (90.9)	0.001*
Interruption of the outer layer	18 (46.2)	29 (87.9)	0.001*
CEUS			
Time to commencement of enhanced†	15 ± 3 (9–23)	15 ± 4 (9–26)	0.646
Washout time(s)†	47 ± 27 (26–125)	30 ± 6 (19–43)	0.008*
Duration of enhancement(s)†	31 ± 27 (10–110)	14 ± 5 (6–24)	0.007*
Tortuous vessels	13 (33.3)	28 (84.8)	<.001*
Early enhancement of adjacent liver	9 (23.1)	2 (6.1)	0.051
Invasion of adjacent liver	2 (5.1)	14 (42.4)	<.001*
Enhancement patterns in arterial phase (inhomogeneous enhanced/homogeneous hyper-enhanced/stratified enhanced)	8/17/14	27/5/1	<.001*
Interruption of the inner layer	7 (17.9)	28 (84.9)	<.001*
Interruption of the outer layer	9 (23.1)	25 (75.8)	<.001*

Unless otherwise indicated, data are number of cases, with percentages in parentheses

† Data are means ± standard deviations, with ranges in parentheses

* $P < 0.05$

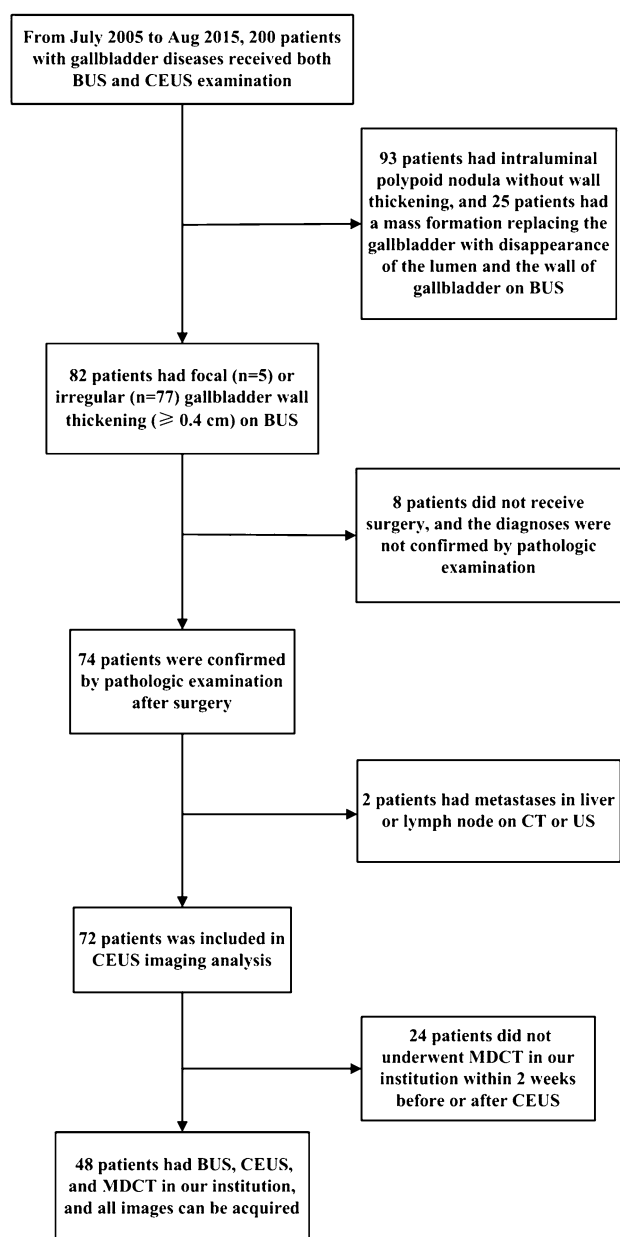


Fig. 1. Flow diagram of the selection of patients.

examination, and all thin slice images can be acquired (Fig. 1).

Imaging techniques

Two series of US equipments were used: (1) Acuson Sequoia 512 (Siemens Medical Solutions, Mountain View, CA), with a 4 V1 vector transducer (frequency range, 1.0–4.0 MHz) and a contrast-specific mode of contrast pulse sequencing (CPS); and (2) Aplio SSA-770 or Aplio 500 (Toshiba Medical Systems, Tokyo, Japan), with a 375BT convex transducer (frequency range, 1.9–6.0 MHz) and a Contrast Harmonic Imaging (CHI)

mode. The mechanical index was <0.1 when contrast-specific imaging modes were initiated in both US systems. Both BUS and CEUS were performed by radiologists (X.Y.X. and X.H.X.), each of whom had at least 5 years of experience in gallbladder CEUS. In each patient, BUS and CEUS examinations were performed by the same radiologist. Each patient underwent fasting at least 8 h before US examination, and a complete BUS scanning of the gallbladder and liver before CEUS. The US contrast agent used in this study was BR1 (SonoVue, Bracco Imaging, Milan, Italy), which consisted of phospholipid-stabilized shell microbubbles filled with sulfur hexafluoride gas. A dose of 2.4 mL of SonoVue was then administered as a bolus via the antecubital vein (within 1–2 s), followed by a flush of 5 mL of 0.9% normal saline using a 20-gauge cannula, and the imaging mode was shifted to the contrast-specific imaging mode at the same time. The transducer was kept in a stable position to record the gallbladder CEUS images continuously for a period of 120 s, without any change in the machine settings. After 120 s, the transducer was moved to scan the liver to exclude liver infiltration or liver metastasis. Different from the liver, the CEUS phases of the gallbladder were classified as the arterial phase (<30 s) and venous phase (31–120 s) [21].

Before MDCT scanning, each patient also underwent fasting at least 8 h. The standard dynamic contrast-enhanced MDCT scan (Aquilion 64; Toshiba Medical System, Tokyo, Japan) procedure was as follows. After an unenhanced helical sequence scan through the liver and gallbladder, arterial and portal venous phase contrast-enhanced CT were performed after 37 and 70 s delay following intravenous administration of 80–100 mL (1.5 mL/kg) of iodinated contrast agent (Ultravist 300; Schering, Berlin, Germany) was administered via the antecubital vein at a rate of 3–4 mL/s. The following CT acquisition parameters were used: 120 kV, 200–250 mAs, collimation: 64×0.5 mm, slice thickness: 0.5 mm, slice increments: 0.5 mm and pitch: 0.9, field of view: 350×350 mm, matrix: 512×512 . Contrast-enhanced CT was reconstructed with reconstruction thickness of 2.5 mm.

Imaging analysis

All of the images were evaluated by two investigators (L.D.C. and Z.W.) who had more than 3 years of experience in gallbladder CEUS, and 5 years of experience in gallbladder BUS and CT independently. Both CEUS and MDCT images of the same patient were reviewed by the same radiologist. In cases of discordance, a third investigator (W.W., with at least 5 years of experience in gallbladder CEUS, BUS, and CT) made the final decision. The investigators were blinded to the final diagnosis, relevant laboratory data, and any clinical manifestation.

On BUS, the thickness of the gallbladder wall was measured. Cholecystolithiasis and the continuity of the inner and outer layers of the gallbladder wall were also recorded. On CEUS, the following features were recorded: (1) time to commencement of enhanced (start from the injection of contrast agent to the beginning of enhancement in the thickened gallbladder wall), washout time (start from the injection of contrast agent to the time when the thickened gallbladder wall became hypo-enhancement compared with the normal liver), and duration of enhancement of the thickened gallbladder wall (=“washout time” - “time to commencement of enhanced”); (2) vascularity in the thickened wall during the arterial phase was classified as tortuous (when the artery was curved and devious), and linear (when the artery was straight and long)/dotted (when the artery was short and speckled) (Fig. 2); (3) invasion of the adjacent liver was defined as hyper-enhancement in the arterial phase followed by hypo-enhancement in the venous phase, with reference to the normal liver tissue; and (4) early enhancement of the adjacent liver referred to transient and earlier hyper-enhancement of the liver adjacent to the gallbladder before the enhancement of the normal liver, and then become iso-enhanced compared with the normal liver in the venous phase. During the contrast imaging period, interrupted inner and outer layers of the gallbladder wall were also evaluated.

The enhancement level of the thickened wall in the arterial phase was divided into hyper-, iso-, and hypo-enhanced compared with the normal liver. The enhancement patterns in the arterial phase were classified as (1) inhomogeneous enhanced; (2) homogeneous enhanced; and (3) stratified enhanced, when the inner and outer layers were hyper-enhanced and the middle layer was hypo-enhanced (Fig. 3).

On MDCT, the following features were recorded: vascularity, invasion of the adjacent liver (assessment using coronal and sagittal reconstructions), enhancement levels and patterns in the arterial phase, and interruption of the inner and outer layers of the gallbladder wall. The diagnostic criteria of gallbladder carcinoma by CT were as follows according to previous references [6, 22, 23]: an irregular thickened wall showed highly inhomogeneous enhancement during the arterial phase, and iso-attenuation or high attenuation in relation to the adjacent hep-

atic parenchyma during the venous phase, with an interruption of the inner or outer layer. The same investigators (L.D.C., Z.W., and W.W.) reviewed all the images to make the final diagnosis within an interval of three weeks after CEUS.

Development and validation of an individualized prediction model

To provide the clinician with a quantitative tool to predict individual probability of malignancy, we built the CEUS nomogram on the basis of multivariable logistic analysis [24, 25]. Multivariable logistic regression analysis began with the following CEUS candidate predictors: wall thickness, washout time, enhancement patterns, and continuity of inner layer. For internal validation, concordance index (C-index) was calculated after bootstrap resampling with 1000 repetitions. Decision curve analysis (DCA) was conducted to determine the clinical usefulness of the nomogram by quantifying the net benefits at different threshold probabilities [26, 27]. The decision curve was also plotted for the model using MDCT.

Statistical analysis

Statistical analysis was performed using SPSS software (version 16.0; SPSS, Chicago, Ill) or MedCalc statistical software (version 13.0; MedCalc Software, Mariakerke, Belgium). Significance was set at a two-tailed *P* value less than 0.05. Based on 72 patients, comparison of the clinical and US characteristics was performed using Chi squared test and independent *t* test for continuous variables. To test the inter-observer variability, two operators (L.D.C. and Z.W.) compared the above CEUS features. The intra-class correlation coefficient (ICC) was categorized as follows: slight, $0 \leq \text{ICC} < 0.20$; fair, $0.21 \leq \text{ICC} < 0.40$; moderate, $0.41 \leq \text{ICC} < 0.60$; substantial, $0.61 \leq \text{ICC} < 0.80$; and almost perfect, $\text{ICC} \geq 0.81$. Multivariate logistic regression analysis with a backward stepwise selection method was performed to select independent variables. Based on 48 patients with both CEUS and MDCT, receiver operating characteristic (ROC) analyses were performed for each significant variable to evaluate the diagnostic performance and obtain the optimal cutoff values. The area under the

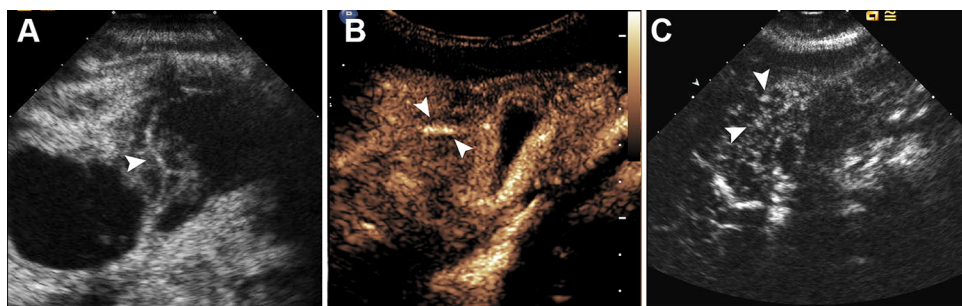


Fig. 2. Vascularity in the thickened gallbladder wall during the arterial phase was classified as tortuous (A), and linear (B)/dotted (C).

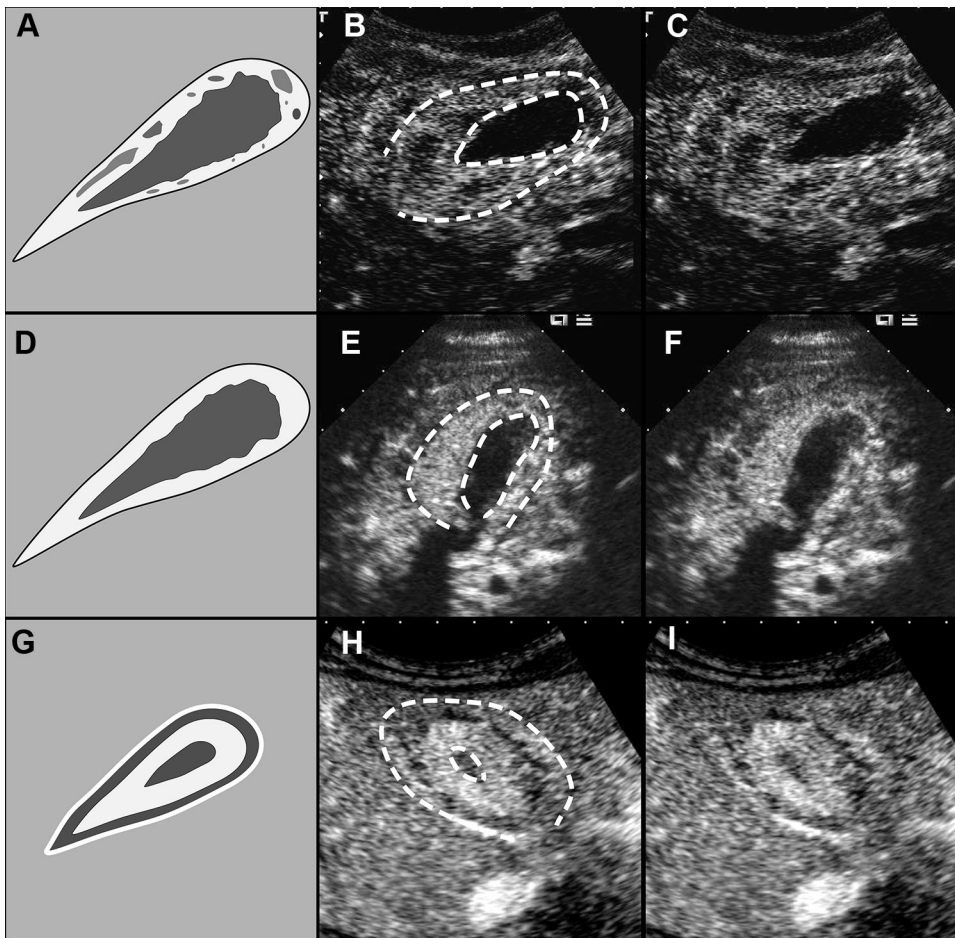


Fig. 3. Three enhancement patterns in arterial phase of CEUS for gallbladder wall thickening diseases: (**A–C**) inhomogeneous enhancement (14 s after injection); (**D–F**) homogeneous enhancement (19 s after injection); and (**G–I**) stratified enhancement (17 s after injection). The schematic images of the three enhancement patterns were showed in **A**, **D**, and **G**. The corresponding pristine images were showed in **C**, **F**, and **I**. The contours of the gallbladder were outlined in **B**, **E**, and **H**.

ROC curve (AUC) was calculated. The diagnostic performance was regarded as low (AUC = 0.5–0.7), moderate (AUC = 0.7–0.9), or high (AUC > 0.9). A nomogram was formulated using the package of “rms” in R version 3.2.5 (<http://www.r-project.org/>). We converted the continuous variables in the nomogram to binary variables based on the optimal cutoff values calculated from the ROC analyses for these variables [28]. Comparisons between the CEUS and MDCT nomogram were performed with the “Hmisc” package in R and were evaluated by the C-index. The larger the C-index, the more accurate was the prognostic prediction. DCA was performed with “dca” package build for R (<http://www.decisioncurveanalysis.org/>).

Results

Patient characteristics

Among the 72 cases, there were 30 gallbladder adenocarcinomas, 23 cholecystitis, 14 adenomyomatosis, 2 adenosquamous carcinomas, 2 abscesses of gallbladder, and 1 squamous cell carcinoma. No significant differences between the benign and malignant groups in gender and CA 19-9. In the malignant group, the ages of patients were older ($P = 0.001$).

Imaging characteristics on BUS

On BUS, the differences of the thickness, and interruption of the inner or outer layer of the gallbladder wall between malignant and benign lesions were statistically significant (all $P < 0.05$, Table 1). There was no significant difference in case of cholecystolithiasis between two groups ($P = 0.291$). Among these patients, 14 cases with adenomyomatosis, negative typical findings of intramural cystic spaces, intramural echogenic foci, and twinkling artifacts were observed on BUS. Also, 2 abscesses of gallbladder did not show obvious colliquative necrosis area in gallbladder fossa.

Multivariate analysis of imaging characteristics on CEUS

WOn CEUS, the ICCs for the CEUS features ranged from 0.737 to 0.938 (Supplementary Table 1), indicating substantial or excellent agreement between the two observers. Early enhancement of the adjacent liver and the enhancement level in the venous phase was classified congruently by each observer independently (ICC = 1.000).

All CEUS features were significantly different between the malignant and benign lesions (all $P < 0.05$,

Table 1), except the time to commencement of enhanced ($P = 0.646$), early enhancement of the adjacent liver ($P = 0.051$). Gallbladder carcinoma was more likely to enhance inhomogeneously with tortuous vessels, and wash out earlier (≤ 40 s); the inner or outer layer was interrupted (Fig. 4). By contrast, the wall in benign gallbladder disease was continuous with layering. The wall of benign disease enhanced homogeneously or stratified with dotted or linear vessels, and the contrast agent washed out later (> 40 s) with longer enhance-

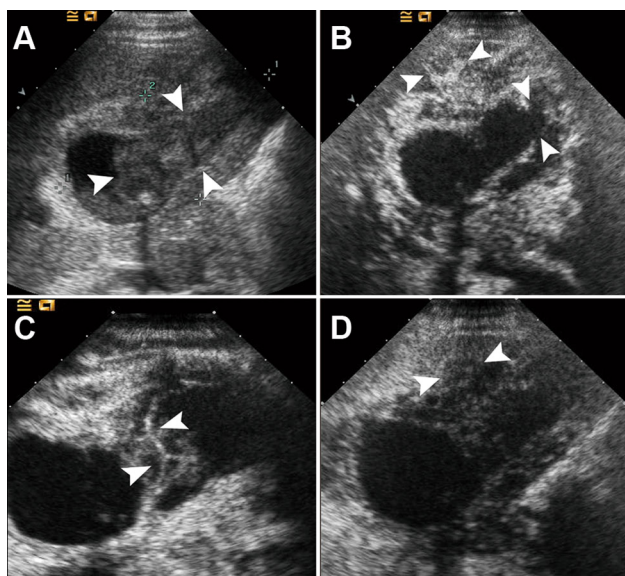


Fig. 4. Images of the gallbladder in a 62-year-old man with moderately differentiated adenocarcinoma. **A** At BUS, a markedly thickened gallbladder wall (maximum thickness = 20 mm) was suspected as malignancy, with hypochoic masses filling in the lumen (*arrowheads*), and unclear boundaries between the masses and gallbladder wall. A gallbladder stone was also noticed. **B** In the arterial phase of CEUS (19 s), the gallbladder wall showed inhomogeneous hyper-enhancement, with disruption of inner and outer layers of the wall (*arrowheads*), and the hyper-enhancing area extending to adjacent liver. CEUS accurately classified this case as a malignant lesion. The intraluminal hypochoic masses detected by BUS were non-enhanced during the whole CEUS examination, and accordingly identified as biliary sludge rather than tumor tissue. **C** Tortuous vessels were detected in the thickened wall (*arrowheads*). **D** The enhancement of the gallbladder wall rapidly turned into hypo-enhanced at 30 s. In the venous phase, the area of the liver being invaded also became hypo-enhanced (*arrowheads*).

ment. Multivariate logistic regression indicated that inhomogeneous enhanced in arterial phase was the strongest independent predictor of malignancy (OR 51.162), followed by interrupted inner layer (OR 19.788), washout time ≤ 40 s (OR 16.686), and wall thickness > 1.6 cm (OR 3.019, Table 2). In the venous phase, all lesions washed out with hypo-enhancing, and the extension of the lesion was clearly depicted.

Comparison of the diagnostic performances of CEUS and MDCT

Among the 24 gallbladder carcinomas who received both CEUS and MDCT scanning, the numbers of cases that displayed malignant features by CEUS were higher than those displayed by MDCT, except for interruption of the outer layer (Table 3). Thus, the AUCs for these features by CEUS (0.690–0.808) were higher than those by MDCT (0.626–0.762). The detection rate of tortuous vessels by CEUS (76.9%) was much higher than that by MDCT (38.5%). The washout time and duration of enhancement were impossible to assess for MDCT because they were not continuously scanned. By CEUS, the enhancement in 84.6% of the malignant lesions washed out before 40 s, and the AUC of this feature reached 0.806. Combining the significant features of CEUS, we developed two sets of diagnostic criteria in predicting malignant gallbladder wall-thickening. When only the two features of inhomogeneous enhanced in arterial phase and interrupted inner layer imaged by CEUS were considered, the AUC of the diagnostic performance for criteria 1 was 0.851, which was higher than that for MDCT (AUC = 0.788). Adding the variable of washout time ≤ 40 s, the diagnostic performance for criteria 2 was improved to high (AUC = 0.917), although the difference between CEUS and MDCT did not reach statistical significance ($P = 0.070$, Table 4). In 8 patients with cholecystitis, 4 of which were complicated by purulent changes, due to the inflammation destroyed the outer layer of gallbladder wall and spreading to adjacent liver, they were misdiagnosed as gallbladder cancer by MDCT. However, these cases showed homogeneous or stratified enhancement in arterial phase and washed out later than 40 s in the venous phase on CEUS, and thus diagnosed correctly by CEUS (Fig. 5). Two patients with cholecystitis were misdiagnosed as malignant lesion by both modalities, because it displayed disruption of the gallbladder wall and washout earlier than 40 s on CEUS.

Table 2. Multivariate logistic regression of the CEUS independent variables in the prediction of malignant gallbladder wall-thickening

Parameter	Coefficient	<i>P</i>	OR	95% CI
Wall thickness > 1.6 cm	1.105	0.397	3.019	0.234, 38.866
Washout time ≤ 40 s	2.815	0.072	16.686	0.781, 356.270
Inhomogeneous enhanced in arterial phase	3.935	0.005	51.162	3.226, 811.290
Interrupted inner layer	2.985	0.034	19.788	1.256, 311.860

Table 3. ROC analysis of CEUS and MDCT features in diagnosing 24 malignant gallbladder wall-thickening patients

Parameter	Number of cases (%)†	Sensitivity	Specificity	NPV	PPV	AUC
CEUS						
Washout time ≤40 s	20 (84.6)	65.0 (40.8, 84.5)	84.0 (63.9, 95.4)	75.0 (55.1, 89.3)	76.5 (50.1, 93.0)	0.806
Duration of enhancement ≤14 s	11 (46.2)	95.0 (75.1, 99.2)	44.0 (24.4, 65.1)	91.7 (61.5, 98.6)	57.6 (39.2, 74.5)	0.743
Tortuous vessels	18 (76.9)	87.5 (67.6, 97.2)	60.7 (40.6, 78.5)	85.0 (62.1, 96.6)	65.6 (46.8, 81.4)	0.741
Invasion of adjacent liver	6 (23.1)	41.7 (22.1, 63.3)	96.4 (81.6, 99.4)	65.9 (49.4, 79.9)	90.9 (58.7, 98.5)	0.690
Inhomogeneous enhanced in arterial phase	22 (92.3)	79.2 (57.8, 92.8)	75.0 (55.1, 89.3)	80.8 (60.6, 93.4)	73.1 (52.2, 88.4)	0.808
Interrupted inner layer	22 (92.3)	79.2 (57.8, 92.8)	82.1 (63.1, 93.9)	82.1 (63.1, 93.9)	79.2 (57.8, 92.8)	0.807
Interrupted outer layer	20 (84.6)	66.7 (44.7, 84.3)	78.6 (59.0, 91.7)	73.3 (54.1, 87.7)	72.7 (49.8, 89.2)	0.726
MDCT						
Tortuous vessels	9 (38.5)	38.5 (14.0, 68.4)	86.7 (59.5, 98.0)	61.9 (38.5, 81.8)	71.4 (29.3, 95.5)	0.626
Invasion of adjacent liver	6 (23.1)	23.1 (5.3, 53.8)	100.0 (78.0, 100.0)	60.0 (38.7, 78.8)	100.0 (30.5, 100.0)	0.615
Inhomogeneous highly enhanced in arterial phase	20 (84.6)	76.9 (46.2, 94.7)	73.3 (44.9, 92.0)	78.6 (49.2, 95.1)	71.4 (41.9, 91.4)	0.749
Interrupted inner layer	18 (76.9)	76.9 (46.2, 94.7)	73.3 (44.9, 92.0)	78.6 (49.2, 95.1)	71.4 (41.9, 91.4)	0.751
Interrupted outer layer	22 (92.3)	92.3 (63.9, 98.7)	60.0 (32.3, 83.6)	90.0 (55.5, 98.3)	66.7 (41.0, 86.6)	0.762

Unless otherwise indicated, data are percentages, with 95% CI in parentheses

† Data are number of cases, with percentages in parentheses

Table 4. Comparison of the diagnostic performances of CEUS and MDCT in differentiation of gallbladder wall-thickening ($n = 48$)

Diagnostic criteria	Sensitivity	Specificity	NPV	PPV	Accuracy	AUC†	P†
CEUS							
Criteria 1	92.0 (73.9, 98.8)	78.3 (56.3, 92.5)	90.0 (68.3, 98.5)	82.1 (63.1, 93.9)	0.854	0.851	0.415 (vs. MDCT)
Criteria 2	92.0 (73.9, 98.8)	87.0 (66.4, 97.2)	90.9 (70.8, 98.9)	88.5 (69.8, 97.6)	0.896	0.895	0.079 (vs. MDCT)
MDCT	84.0 (63.9, 95.5)	69.6 (47.1, 86.7)	80.0 (56.3, 94.3)	75.0 (55.1, 89.3)	0.792	0.768	
BUS	87.5 (67.6, 97.2)	46.4 (27.5, 66.1)	81.2 (54.3, 95.7)	58.3 (40.8, 74.5)	0.654	0.670	0.011 (vs. Criteria 2)

Unless otherwise indicated, data are percentages, with 95% CI in parentheses

Criteria 1: Interrupted inner layer, or inhomogeneous enhancement in arterial phase

Criteria 2: Meet any two of the following three conditions: Interrupted inner layer, inhomogeneous enhancement in arterial phase, and washout time ≤40 s

† Data are raw data

Two adenosquamous carcinomas were misdiagnosed by CEUS or MDCT due to their atypical hypo-enhancement during the arterial and venous phase.

Development and validation of an individualized prediction model using CEUS

The model that incorporated the above independent predictors was developed and presented as the nomogram (Fig. 6). The C-index for the prediction nomogram was 0.974, which was confirmed to be 0.950 via bootstrapping internal validation. The C-index of MDCT nomogram was 0.827. The decision curve analysis for the CEUS and MDCT nomograms was presented in Fig. 7. The decision curve showed that using the CEUS nomogram to predict malignancy adds more benefit than either the treat-all-patients scheme or the treat-none scheme. Within this range, net benefit of CEUS nomogram was better than the model using MDCT.

Discussion

Gallbladder wall thickening is very common in not only gallbladder neoplasms but also extra-cholecystic conditions. Only those cases suspected to be carcinomas by

BUS imaging need to be further investigated. By BUS, the coexistence of inflammatory or fibrotic changes, gallstones or bile sludge, as well as tumor tissue, can produce similar imaging characteristics. By CEUS, owing to the strong tissue contrast, the non-enhancing gallstones or bile sludge, hypo-enhancing fibrotic tissues, and the hyper-enhancing contours of the gallbladder wall layers and liver parenchyma could be clearly discriminated. The application of trans-abdominal CEUS in the gallbladder occurred early in 2002 [18]. The results showed limited value in the differentiation of gallbladder disease. However, the static contrast technique is insensitive to slow flow and deeply located vessels. By using the second-generation contrast agent of SonoVue, CEUS achieved real-time depiction of the microcirculation of gallbladder diseases. The results of several studies [5, 17, 19, 29] indicated that CEUS is valuable in differentiating malignant from benign gallbladder diseases. However, most of these studies focused on polypoid lesions of the gallbladder, and no study has assessed the value of CEUS compared with CT.

In this study, we found that wall thickness >1.6 cm, interrupted inner layer, inhomogeneous enhanced in arterial phase, and washout time ≤40 s were predictors of

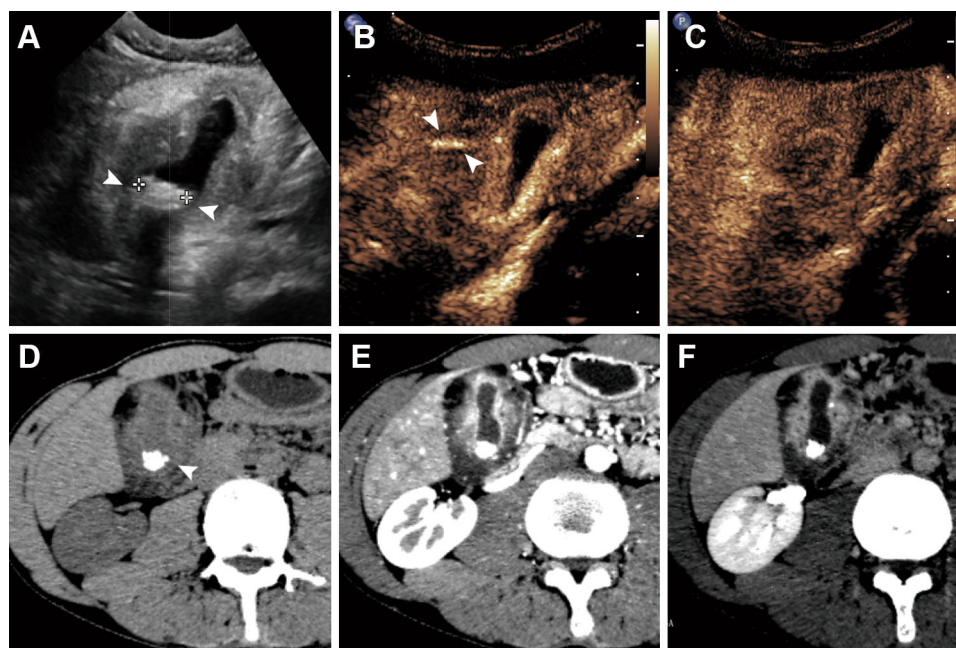


Fig. 5. Images of the gallbladder in a 36-year-old woman with chronic cholecystitis. **A** At BUS, a markedly thickened gallbladder wall (maximum thickness = 24 mm) was suspected as malignancy. A gallbladder stone was also noticed (*arrowheads*). **B** In the arterial phase of CEUS (17 s), stratified enhancement was observed with a linear artery in the gallbladder wall (*arrowheads*). **C** The enhancement of the gallbladder wall began to wash out at 81 s, and remained hypo-enhancement during the venous phase. This patient

was classified as a benign wall-thickening according to our diagnostic criteria of CEUS. **D** On unenhanced CT, the gallbladder wall was irregularly thickened with a stone in the lumen (*arrowheads*), **E** it showed highly inhomogeneous enhancement in the arterial phase, with an interruption of the outer layer, **F** and high attenuation in the venous phase. This patient was diagnosed as gallbladder cancer by MDCT scanning.

malignancy. By contrast, the wall of a benign disease such as cholecystitis was uniformly thickened, with continuous layering; the contrast agent washed out later. In our opinion, the intercostal or subcostal scanning of CEUS can obtain sections along the long axis of the gallbladder. This unique scanning plane is superior in its ability to detect the continuity of the inner and outer wall as well as the symmetry of the gallbladder wall. In addition to free plane scanning, real-time data acquisition is another advantage of CEUS over CT. As we expected, hyper-enhancement in the arterial phase and washout in the venous phase does not indicate gallbladder malignancy. However, we could identify the time point of washout during real-time scanning. Washout time ≤ 40 s was one of the independent variables of CEUS in predicting malignant wall thickening. This feature is unavailable for CT scanning. Moreover, real-time scanning could delineate detailed enhancement patterns. The inhomogeneous enhancement patterns for malignancy were different with inflammation, which is homogeneous hyper-enhancement or stratified enhancement with layering. Additionally, real-time CEUS can capture the temporal moment of lesion vascularity. Tortuous vessels were observed much more in carcinomas than in benign lesions. Due to the hyper-vascularity

in most gallbladder carcinomas, the blood supply of the tumor is often dilated and distorted. Tortuous intralésional vessels and the destruction of the gallbladder wall are the features highly suggestive of malignancy.

Xu, J. M. et al. [29] found that outer wall discontinuity is also a diagnostic clue for malignancy. However, we observed 8 cholecystitis or abscess patients in our series. Interruption of the gallbladder wall could occur not only with destruction by malignant tumors but also with perforation by acute or chronic inflammation. As a result, discontinuity of the outer layer failed to be included among the significant independent variables by logistic regression analysis.

By MDCT, most gallbladder carcinomas showed inhomogeneous high enhancement in the arterial phase, irregular wall thickening, and interruption of the gallbladder wall, findings that were in accordance with those of previous reports [4, 22, 23, 30]. Compared with MDCT, the detection rates of malignant features in gallbladder carcinoma were all higher by CEUS, especially the delineation of blood vessels. When the above advantages of CEUS were added, the diagnostic efficacy of CEUS was higher than that of MDCT. Eight (16.7%) cases with cholecystitis suspected as malignancy by both BUS and MDCT were correctly diagnosed by CEUS due

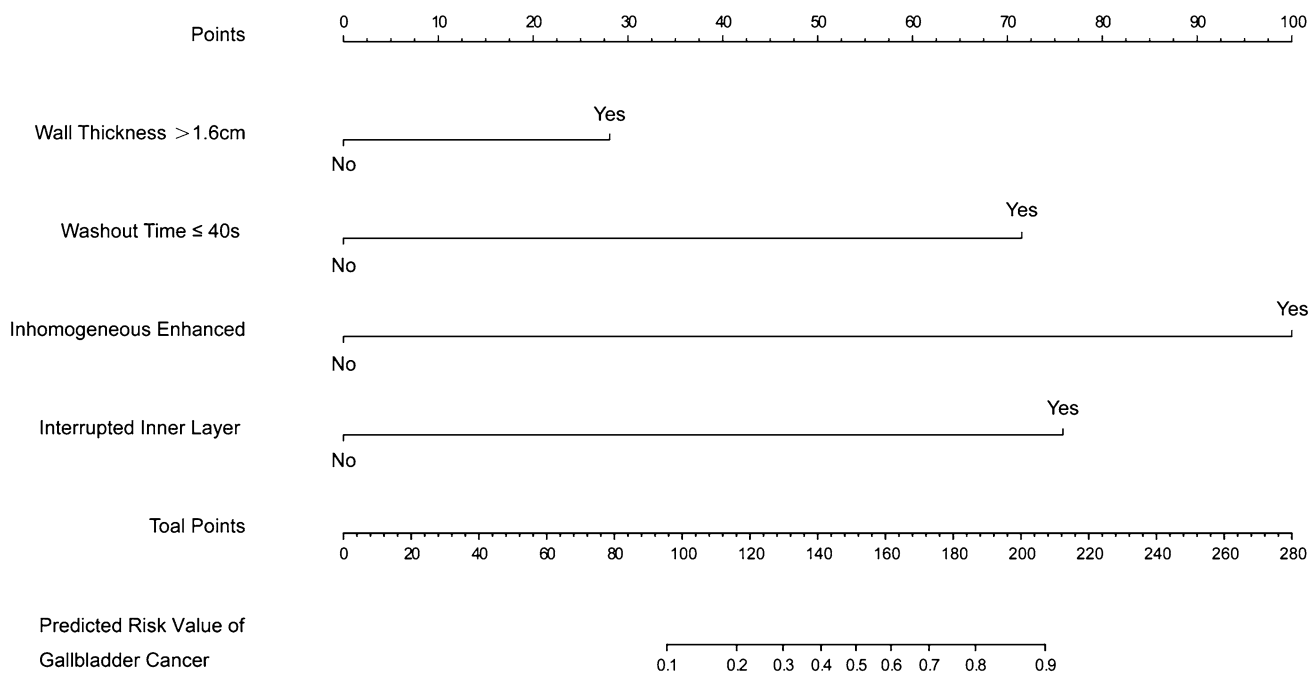


Fig. 6. CEUS-based nomogram for the preoperative individualized prediction of malignancy in patients with gallbladder wall thickening. An individual patient’s value was located on each variable axis, and a line is drawn upward to determine

the number of points received. The sum of these numbers is located on the Total Points axis, and a line is drawn downward to the bottom scale to determine the likelihood of malignancy.

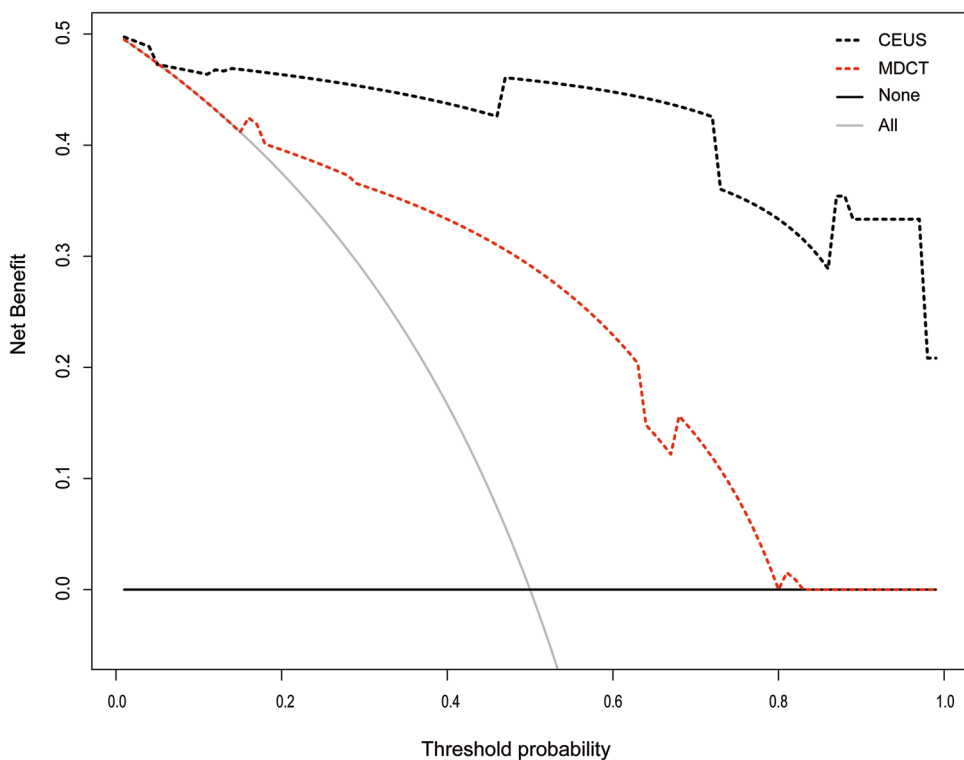


Fig. 7. Decision curve analysis for the nomograms. The *black-* and *red-dotted lines* represented the CEUS and MDCT nomograms, respectively. The *black solid line* represents the assumption that all patients were malignancy. Thin *gray solid line* represents the assumption that no patients were malignancy. The y-axis measures the net benefit, which was calculated by subtracting the proportion of all patients who are false positive from the proportion who are true positive, weighting by the relative harm of forgoing treatment compared with the negative consequences of an unnecessary treatment [27].

to their specific enhancement patterns and evaluation of dynamic enhancement time. Therefore, surgical resection should have been avoided in these patients.

We developed and validated a diagnostic nomogram using CEUS for the preoperative individualized prediction of malignancy in patients with irregular gallbladder

wall thickening. This easy-to-use nomogram achieved satisfactory discrimination (C-index, 0.974, and 0.950 in internal validations) [24, 25]. To justify the clinical usefulness, decision curve analysis was applied to assess whether the nomogram would improve patient outcomes. This novel method offers net benefits to evaluate clinical consequences on the basis of threshold probability. The decision curve showed that using the CEUS nomogram in the current study added more benefit than either the treat-all-patients scheme or the treat-none scheme or the model using MDCT [24, 26]. Therefore, CEUS could have led to more accurate treatment plans and beneficial to patient prognosis. Considering the US advantages of imaging in real time, ease of use, cost effectiveness, no ionizing radiation, and US contrast agents being relatively harmless with a low incidence of side effects and without nephrotoxicity [31], CEUS can establish its status in the differentiation of irregular wall-thickened gallbladder diseases.

Our study has some limitations. First, the proportion of cases between malignant and benign gallbladder wall thickening was different with that in routine clinical works. Most benign cases, for example, those caused by renal failure, heart failure, and hypoproteinemia, were not included. This could lead to a selection bias when calculating the positive and negative predictive values. Second, quantitative analyses of time-intensity curve, such as time to peak, peak intensity, ascending slope, and descending slope should be measured using specific software instead of subjective observation. More features might be helpful for discrimination. Third, the number of cases in the study group was relatively small; thus, a multi-center study with a larger sample is necessary in the future.

Conclusions

CEUS could accurately differentiate between malignant and benign gallbladder wall thickening with equivalent efficacy compared to MDCT, and thus may lead to accurate treatment plans and beneficial to patient prognosis. The proposed nomogram could be conveniently used to facilitate the preoperative individualized prediction of malignancy in patients with irregular gallbladder wall thickening.

Compliance with ethical standards

Funding This study was funded by the National Nature Science Foundation of China (No: 81301238), Guangdong Science and Technology Foundation (NO.:2016A020215042), Guangdong Medical Scientific Research Foundation (NO. 201611610484333).

Conflict of interest The authors declare that they have no conflict of interest.

Ethical approval All procedures performed in studies involving human participants were in accordance with the ethical standards of the institutional and/or national research committee and with the 1964

Helsinki declaration and its later amendments or comparable ethical standards.

Informed consent Informed consent was obtained from all individual participants included in the study.

References

1. D'Hondt M, Lapointe R, Benamira Z, et al. (2013) Carcinoma of the gallbladder: patterns of presentation, prognostic factors and survival rate. An 11-year single centre experience. *Eur J Surg Oncol* 39(6):548–553
2. Miller G, Jarnagin WR (2008) Gallbladder carcinoma. *Eur J Surg Oncol* 34(3):306–312
3. Vijayakumar A, Vijayakumar A, Patil V, et al. (2013) Early diagnosis of gallbladder carcinoma: an algorithm approach. *ISRN Radiol* 2013:239424
4. van Breda Vriesman AC, Engelbrecht MR, Smithuis RH, et al. (2007) Diffuse gallbladder wall thickening: differential diagnosis. *AJR Am J Roentgenol* 188(2):495–501
5. Meacock LM, Sellars ME, Sidhu PS (2010) Evaluation of gallbladder and biliary duct disease using microbubble contrast-enhanced ultrasound. *Br J Radiol* 83(991):615–627
6. Runner GJ, Corwin MT, Siewert B, et al. (2014) Gallbladder wall thickening. *AJR Am J Roentgenol* 202(1):W1–W12
7. Kim BS, Oh JY, Nam KJ, et al. (2014) Focal thickening at the fundus of the gallbladder: computed tomography differentiation of fundal type adenomyomatosis and localized chronic cholecystitis. *Gut Liver* 8(2):219–223
8. Dutta U (2012) Gallbladder cancer: can newer insights improve the outcome? *J Gastroenterol Hepatol* 27(4):642–653
9. Imazu H, Mori N, Kanazawa K, et al. (2014) Contrast-enhanced harmonic endoscopic ultrasonography in the differential diagnosis of gallbladder wall thickening. *Dig Dis Sci* 59(8):1909–1916
10. Park CH, Chung MJ, Oh TG, et al. (2013) Differential diagnosis between gallbladder adenomas and cholesterol polyps on contrast-enhanced harmonic endoscopic ultrasonography. *Surg Endosc* 27(4):1414–1421
11. Jang JY, Kim SW, Lee SE, et al. (2009) Differential diagnostic and staging accuracies of high resolution ultrasonography, endoscopic ultrasonography, and multidetector computed tomography for gallbladder polypoid lesions and gallbladder cancer. *Ann Surg* 250(6):943–949
12. Park KW, Kim SH, Choi SH, et al. (2010) Differentiation of nonneoplastic and neoplastic gallbladder polyps 1 cm or bigger with multi-detector row computed tomography. *J Comput Assist Tomogr* 34(1):135–139
13. Song ER, Chung WS, Jang HY, et al. (2014) CT differentiation of 1-2-cm gallbladder polyps: benign vs malignant. *Abdom Imaging* 39(2):334–341
14. Inoue T, Kitano M, Kudo M, et al. (2007) Diagnosis of gallbladder diseases by contrast-enhanced phase-inversion harmonic ultrasonography. *Ultrasound Med Biol* 33(3):353–361
15. Xie XH, Xu HX, Xie XY, et al. (2010) Differential diagnosis between benign and malignant gallbladder diseases with real-time contrast-enhanced ultrasound. *Eur Radiol* 20(1):239–248
16. Adamietz B, Wenkel E, Uder M, et al. (2007) Contrast enhanced sonography of the gallbladder: a tool in the diagnosis of cholecystitis? *Eur J Radiol* 61(2):262–266
17. Liu LN, Xu HX, Lu MD, et al. (2012) Contrast-enhanced ultrasound in the diagnosis of gallbladder diseases: a multi-center experience. *PLOS ONE* 7(10):e48371
18. Kim KA, Park CM, Park SW, et al. (2002) Contrast-enhanced power Doppler US: is it useful in the differentiation of gallbladder disease? *Clin Imaging* 26(5):319–324
19. Numata K, Oka H, Morimoto M, et al. (2007) Differential diagnosis of gallbladder diseases with contrast-enhanced harmonic gray scale ultrasonography. *J Ultrasound Med* 26(6):763–774
20. Claudon M, Dietrich CF, Choi BI, et al. (2013) Guidelines and good clinical practice recommendations for Contrast Enhanced Ultrasound (CEUS) in the liver—update 2012: A WFUMB-EF-SUMB initiative in cooperation with representatives of AFSUMB, AIUM, ASUM, FLAUS and ICUS. *Ultrasound Med Biol* 39(2):187–210

21. Claudon M, Cosgrove D, Albrecht T, et al. (2008) Guidelines and good clinical practice recommendations for contrast enhanced ultrasound (CEUS)—update 2008. *Ultraschall Med* 29(1):28–44
22. Yun EJ, Cho SG, Park S, et al. (2004) Gallbladder carcinoma and chronic cholecystitis: differentiation with two-phase spiral CT. *Abdom Imaging* 29(1):102–108
23. Kim SJ, Lee JM, Lee JY, et al. (2008) Analysis of enhancement pattern of flat gallbladder wall thickening on MDCT to differentiate gallbladder cancer from cholecystitis. *AJR Am J Roentgenol* 191(3):765–771
24. Huang YQ, Liang CH, He L, et al. (2016) Development and validation of a radiomics nomogram for preoperative prediction of lymph node metastasis in colorectal cancer. *J Clin Oncol* 34:2157–2164
25. Wang Y, Li J, Xia Y, et al. (2013) Prognostic nomogram for intrahepatic cholangiocarcinoma after partial hepatectomy. *J Clin Oncol* 31(9):1188–1195
26. Vickers AJ, Elkin EB (2006) Decision curve analysis: a novel method for evaluating prediction models. *Med Decis Making* 26(6):565–574
27. Vickers AJ, Cronin AM, Elkin EB, et al. (2008) Extensions to decision curve analysis, a novel method for evaluating diagnostic tests, prediction models and molecular markers. *BMC Med Inform Decis Mak* 8:53
28. Zhang JX, Song W, Chen ZH, et al. (2013) Prognostic and predictive value of a microRNA signature in stage II colon cancer: a microRNA expression analysis. *Lancet Oncol* 14(13):1295–1306
29. Xu JM, Guo LH, Xu HX, et al. (2014) Differential diagnosis of gallbladder wall thickening: the usefulness of contrast-enhanced ultrasound. *Ultrasound Med Biol* 40(12):2794–2804
30. Zissin R, Osadchy A, Shapiro-Feinberg M, et al. (2003) CT of a thickened-wall gall bladder. *Br J Radiol* 76(902):137–143
31. Bokor D, Chambers JB, Rees PJ, et al. (2001) Clinical safety of SonoVue, a new contrast agent for ultrasound imaging, in healthy volunteers and in patients with chronic obstructive pulmonary disease. *Invest Radiol* 36(2):104–109